An analysis system for PET detector

Hong-Chih Liu, Hsing-Ching Liang

Institute of Nuclear Energy Research, P. O. Box 3-4, Lung-Tan,
Taiwan, Republic of China

ABSTRACT

The ASR-PET detector is designed by coupling a 7×8 array of BGO scintillation crystals to a PSPMT (Position Sensitive Photo-Multiplier Tube). Reflectors between the crystals confine the light from a gamma ray interaction and control the distribution of light to the PSPMT. The output signals of the PSPMT are used to identify the crystal of scintillation and the energy being released from the gamma ray interaction.

The subject of this study is to generate a LUT (Lookup Table) from the position response distribution of the block detector and to analyze the PHS (Pulse Height Spectrum) of each crystal. By combining the image-processing and neural network data fitting techniques, this system gives a flexible, user-friendly and powerful approach to perform the analysis with satisfactory accuracy.

Keywords: PET, Block detector.

1. INTRODUCTION

In most PET system, BGO block detectors[1-6] are used to detect coincident 511Kev gamma rays resulting from positron annihilations. In the ASR-PET (designed by the Institute of Nuclear Energy Research, Taiwan, Republic of China), each BGO block detector module consists of a 7 × 8 BGO array coupled to the compact PSPMT (Position Sensitive Photo-Multiplier Tube). Reflectors between the crystals confine the light from a gamma ray interaction and control the distribution of light to the PSPMT. The PSPMT output signals are decoded into transaxial (x) and axial (y) position information. The summation of the PSPMT output signals is transformed into energy information.

The subject of this study is to generate a LUT (Lookup Table) from the position response distribution of the block detector and to analyze the PHS (Pulse Height Spectrum) of each crystal. The ASR-PET block detector and data acquisition system is briefly described in section 2, while the detail of LUT and PHA algorithms are presented in section 3 and 4. A conclusion is given in section 5.

2. THE ASR-PET BLOCK DETECTORS AND DATA ACQUISITION SYSTEM

The ASR-PET block detector module consists of a 7 × 8 BGO array coupled to the compact PSPMT (Hamamatsu R5900-00-C8) as shown in Figure 1. The dimensions of each BGO crystal are 2.6 mm in width, 2.6 mm in height and 25 mm in depth. Crystals are painted with reflection material and closely packed. Reflectors between the crystals confine the light from a gamma ray interaction and control the distribution of light to the PSPMT. The PSPMT has metal channel dynodes and 8 cross plate anodes (4 for X dimension and 4 for Y dimension). These anodes output signals can be used to determine the location of the scintillation event. The total summation of these anode signals can also provide information of the energy of the scintillation event.

The hardware used for data acquisition is shown in Figure 2. The signals from 8 anodes of PSPMT are independently amplified through preamplifiers (LeCroy 612AM Fast Preamplifier) and offset-compensated by Fan-in/Fan-out modules (LeCroy 428F Linear Fan-in/Fan-out). The sum of these eight PMT signals is filtered (ORTEC 474 Timing Filter Amplifier), threshold (LeCroy 4608C Discriminator) and gated (LeCroy 222 Gate Generator) before it can be sent to trigger the ADC module. A delay device is inserted between each output of the preamplifier and the input of the charge integrating ADC to compensate the timing delay introduced by the trigger module. The digitized signals captured by the ADC (LeCroy 4300 Fast Encoding/Readout ADC) are recorded and further processed by LUT and PHS analysis programs.

In *Optical Sensing, Imaging, and Manipulation for Biological and Biomedical Applications*, Robert R. Alfano, Ping-Pei Ho, Arthur E. T. Chiou, Editors, Proceedings of SPIE Vol. 4082 (2000) • 0277-786X/00/$15.00

3. LUT GENERATION ALGORITHM AND RESULTS

The LUT generation program is developed under Borland C++ Builder. In Figure 3, flow diagram of the LUT generation algorithm is shown. The LUT generation algorithm use the PSPMT anode signals to identify the crystal of scintillation. For each gamma ray interaction, the measured position value (X_m, Y_m) from these signals are calculated by:

$$X_m = \frac{3X_1 + X_2 - X_3 - 3X_4}{X_1 + X_2 + X_3 + X_4}$$

$$Y_m = \frac{3Y_1 + Y_2 - Y_3 - 3Y_4}{Y_1 + Y_2 + Y_3 + Y_4}$$

where X_1, X_2, X_3, X_4 and Y_1, Y_2, Y_3, Y_4 are the amplified anodes signals captured by the ADCs. The relationship between the measured position and the true position is nonlinear in both X and Y positions. The LUT generation algorithm is designed to identify the crystal of interaction corresponding to a given (X_m, Y_m) pairs.

Figure 4(a) shows the intermediate output of the LUT generation algorithm. A 256×256 position response distribution is obtained from the flood source (Na^{22}) measurement. There is a distinct peak in the distribution for each crystal in the position response distribution. The lookup table is generated for each detector from its flood source response such that every possible (X_m, Y_m) pair will be assigned to one crystal and no detected events are thrown away. The region of each crystal occupied is assumed to have a boundary of four-sided polygons[3], since it is easy to generate and flexible to bound the 56 crystal position peaks. Figure 4(c) shows the 2-D position response distribution after smoothing and energy threshold. Figure 4(d) gives the LUT boundaries overlaid on the original position response distribution.

Large peak-to-valley ratios are desirable for block detectors. Large ratios mean the peaks are well separated and thus identification the crystals of interaction are correct for a large fraction of the events. Figure 5(a) shows two areas (each with 10 pixels wide on a 256×256 image) marked across BGO crystal array and their relative position profiles are shown in Figure 5(b). Even after averaging across 10 pixels, the separations between the peaks are still acceptable. Figure 5(c) and (d) shows the results of two thin lines (each with 2 pixels wide on a 256×256 image) drawn across BGO crystal arrays and their profiles.

4. PHS ANALYSIS ALGORITHM AND RESULTS

Figure 6 shows the coarse energy spectrum of an ASR-PET block detector being exposed to the Na^{22} flood source. The poor energy spectrum may results from the gain variation within the PSPMT and the inconsistent physical contact between the crystal and the PSPMT surface.

In order to overcome the problem of non-uniformity of energy resolution and gamma ray detection efficiency of each BGO crystal, the PHS algorithm is designed to analysis the energy spectrum of each individual BGO crystal. PHS analysis algorithm first calculate the (X_m, Y_m) for each event collected, it then determine which crystal the interaction occurred in, using the LUT generated earlier, and histogram the energy of the every event into one of 56 arrays. In this manner an energy spectrum can be obtained for each crystal. Figure 7 shows the energy spectra of each BGO crystal being exposed to Na^{22} flood source. Using the 56 energy spectra, PHS analysis algorithm approximates gaussian function on each energy peak by artificial neural network data fitting technique. Figure 8 displays results of several BGO crystal energy spectra being approximated by gaussian functions.

In order to observe the 511 keV photopeak detection efficiency of each BGO crystal, PHS analysis algorithm estimates the relative detection efficiency by comparison the area of gaussian function approximation of each 511 keV photopeak. Figure 9 shows the distribution of the number of 511 keV photopeak detected in each crystal of an ASR-PET detector. The counts of the left row are about 20% less than the counts of the central row. These loss counts are believed to be due to the insufficient effective area of the PSPMT surface.

5. SUMMARY

The prime motivation for this study is to conduct a comprehensive and quantitative evaluation of the performance of the BGO block detectors. The LUT algorithm creates the look-up table of each BGO block detectors based on the image-

processing technique. Using the artificial neural network data fitting technique, the PHS analysis algorithm provides a means of observing the 511 keV photopeak detection efficiency. More work will be needed to extend the proposed algorithm to analysis other types of PET detector.

REFERENCES

1. M.E. Casey and R. Nutt, "A multicrystal two dimensional BGO detector system for positron emission tomography", IEEE Trans Nucl Sci, Volume 33, 1986.
2. M. Dahlbom and E.J. Hoffman, "An evaluation of a two-dimensional array detector for high resolution PET", IEEE Trans Med Imaging, Volume 7, 1988.
3. J.G. Rogers, A. J. Taylor, M. F. Rahimi, R. Nutt, M. Andreaco and C.W. Williams, "An improved multicrystal 2-D BGO detector for PET", IEEE Trans Nucl Sci, Volume 39, 1992.
4. M.P. Tornai, G. Germano and E.J. Hoffman, "Positioning and energy response of PET block detectors with different light sharing schemes", IEEE Trans Nucl Sci, Volume 41, 1994.
5. M. Watanabe, T. Omura, H. Kyushima, Y. Hasegawa and T. Yamashita, "A compact position-sensitive detector for PET", IEEE Trans Nucl Sci, Volume 42, 1995.
6. M. Watanabe, H. Okada, K. Shimizu, T. Omura, E. Yoshikawa, T. Kosugi, S. Mori and and T. Yamashita, "A high resolution animal PET scanner using compact PSPMT detectors", IEEE Trans Nucl Sci, Volume 43, 1996.

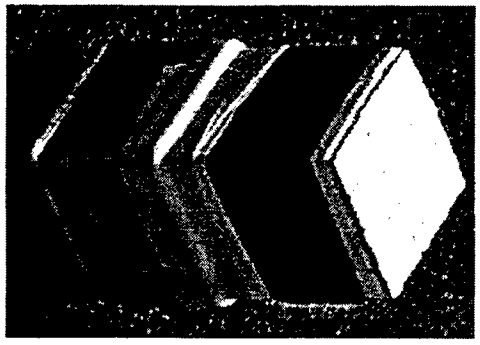

Figure 1. ASR-PET block detector.

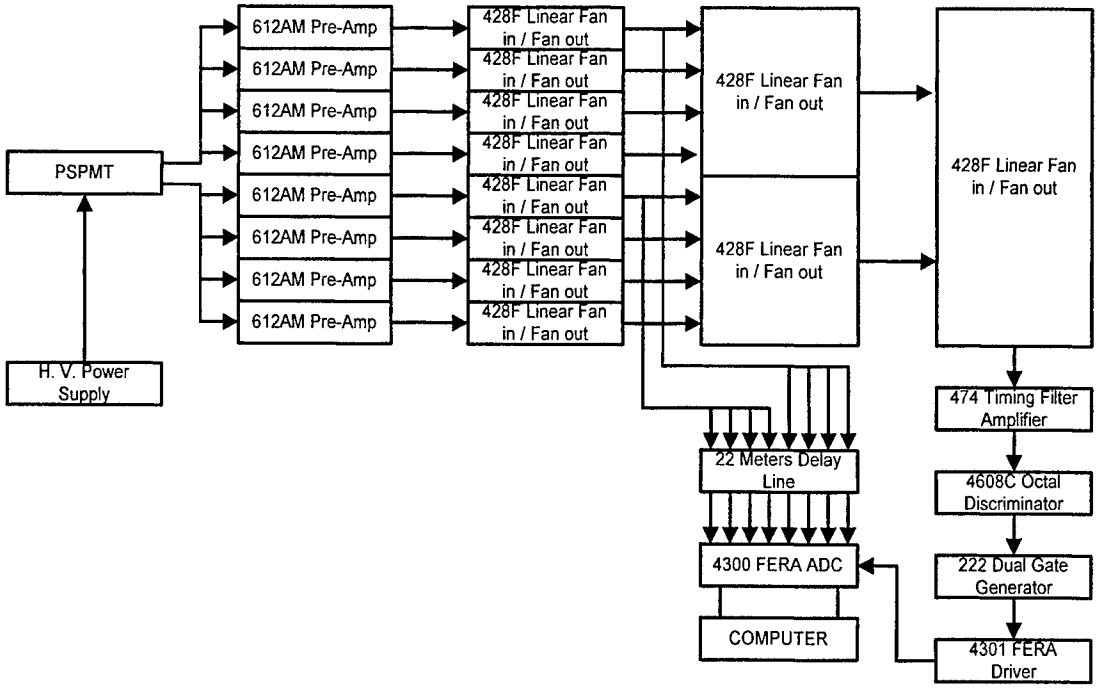

Figure 2. CAMAC modules used for data acquisition.

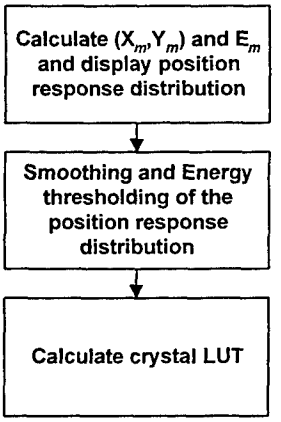

Figure 3. Flow diagram of the LUT generation algorithm

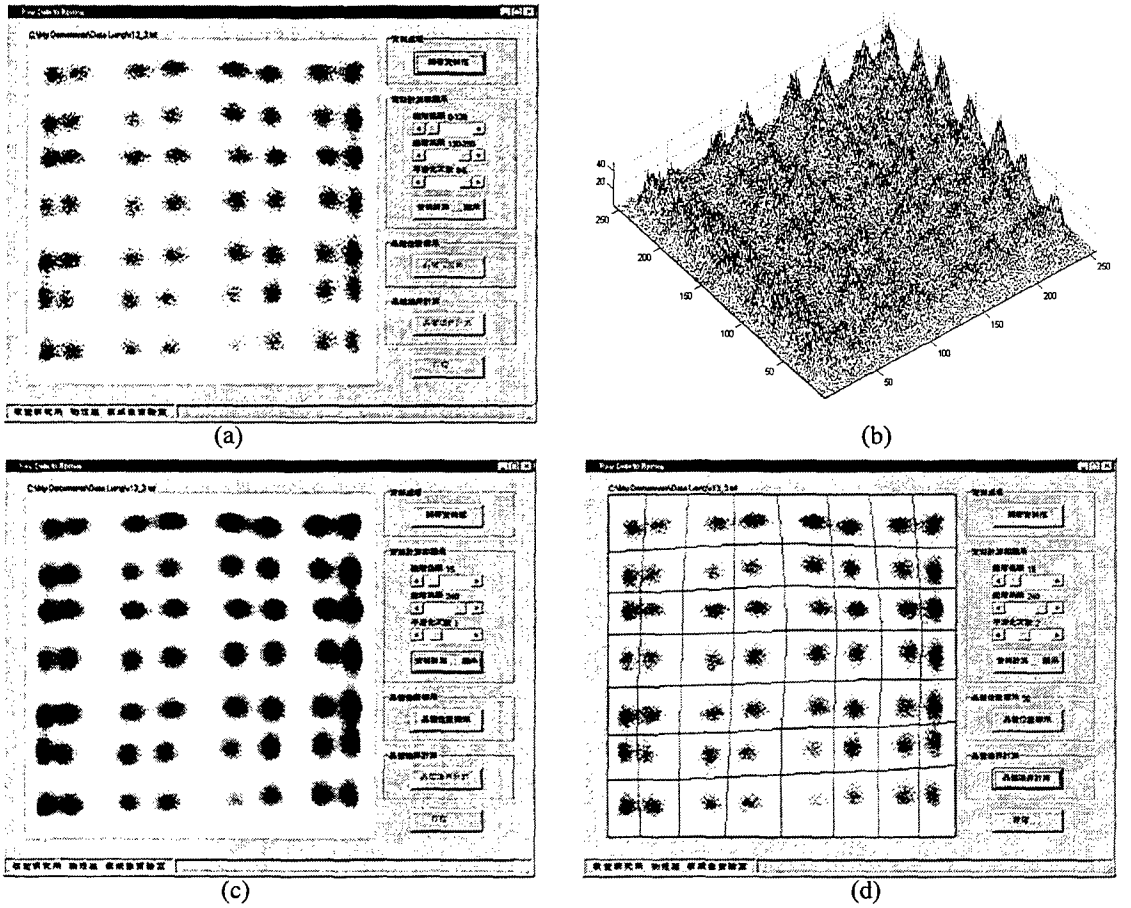

Figure 4. (a) 2-D position distribution of an ASR-PET block detector. (b) 3-D position distribution of an ASR-PET block detector. (c) 2-D position distribution after smoothing and energy thresholding. (d) 2-D position distribution with LUT overlaid.

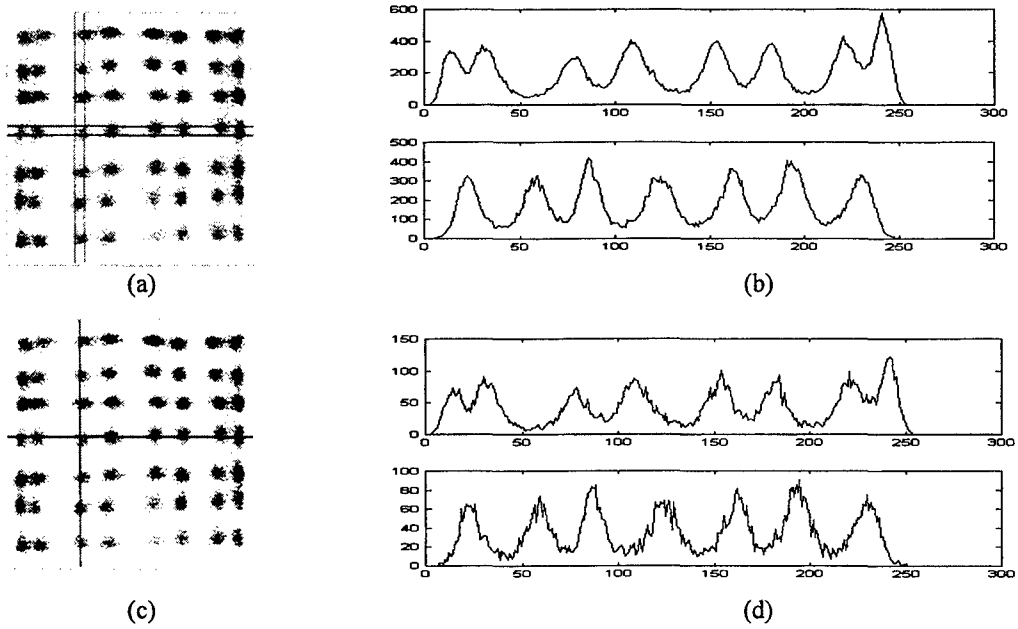

Figure 5. (a) 2-D position distribution with two thick areas overlaid (b) Result profiles of (a). (See text for details.) (c) 2-D position distribution with two thin lines overlaid (d) Result profiles of (c).

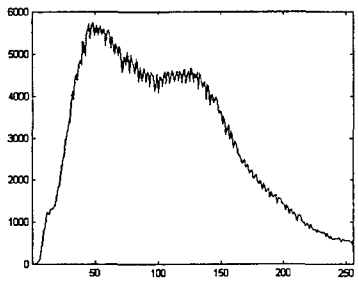

Figure 6. Coarse energy spectrum of an ASR-PET block detector being exposed to the Na^{22} flood source.

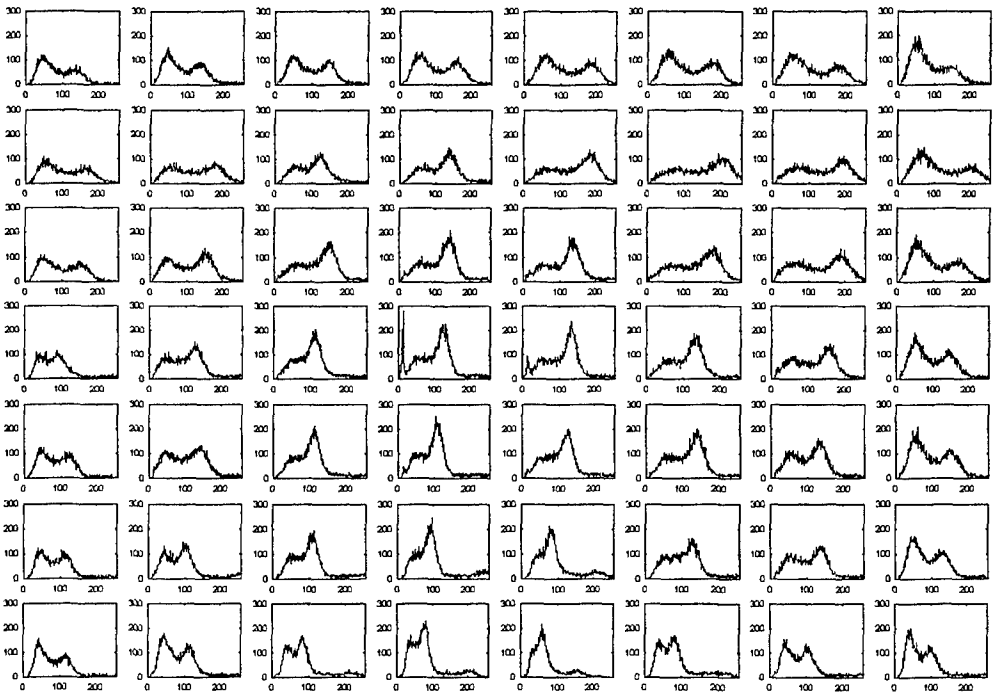

Figure 7. Pulse height spectra (PHS) of each BGO crystal exposed to Na^{22} flood source.

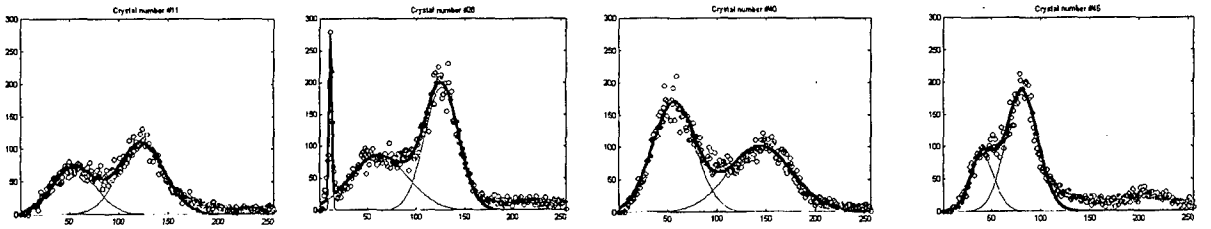

Figure 8. Examples of the individual BGO crystal energy spectra (denoted by small circles) and their approximation of gaussian functions (denoted by solid lines).

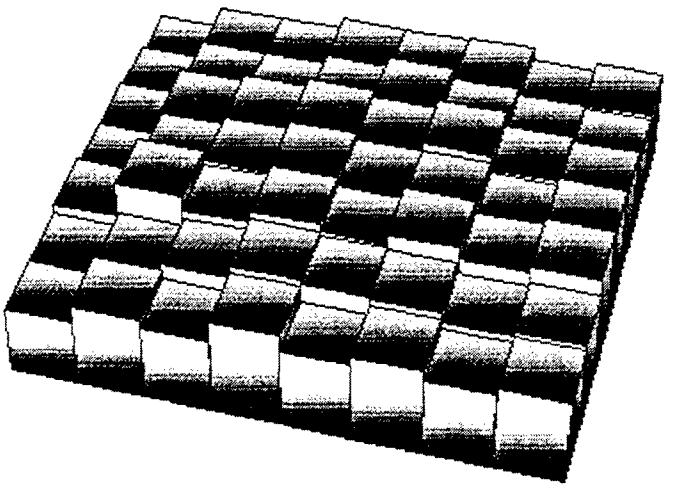

Figure 9. Relative 511 keV detection efficiency across the detector.